ISSN 1063-7834, Physics of the Solid State, 2015, Vol. 57, No. 5, pp. 983–991. © Pleiades Publishing, Ltd., 2015.
Original Russian Text © V.S. Zhandun, V.I. Zinenko, 2015, published in Fizika Tverdogo Tela, 2015, Vol. 57, No. 5, pp. 970–977.

LATTICE DYNAMICS

Ab Initio Investigation of the Magnetic and Ferroelectric Properties of Double Perovskites LaPb*Me*SbO$_6$ (*Me* = Mn, Fe, Co, Ni)

V. S. Zhandun* and V. I. Zinenko

Kirensky Institute of Physics, Siberian Branch of the Russian Academy of Sciences, Akademgorodok 50–38, Krasnoyarsk, 660036 Russia

* *e-mail: jvc@iph.krasn.ru*

Received November 5, 2014

Abstract—The results of ab initio calculations of the ferroelectric and magnetic properties of the recently synthesized double perovskites LaPb*Me*SbO$_6$ (Me^{2+} = Mn^{2+}, Fe^{2+}, Co^{2+}, Ni^{2+}) have been presented. The ordered double perovskites with a layered ordering of cations *A* and *A*' and a checkerboard ordering of cations *B* and *B*' have been considered. The calculation of the lattice dynamics has revealed instabilities in the phonon spectra of the high-symmetry phase of these compounds. The condensation of unstable modes leads to a stable polar phase $P2_1$. The spontaneous polarization in this phase is found to be ~30 μC/cm^2. The magnetic ground state is antiferromagnetic with an antiparallel direction of the magnetic moments in adjacent planes along the [001] direction. The Néel temperatures are estimated in the mean field approximation. The presence of the ferroelectric and magnetic order parameters in the structure suggests that the studied double perovskites with the simultaneous ordering of the cations are potential multiferroics.

DOI: 10.1134/S1063783415050340

1. INTRODUCTION

Double perovskites of the general formula $AA'BB'O_6$ have recently attracted considerable interest due to the wide variety of their physical properties, which depend on the chemical composition of the cations *A, A*', *B*, and *B*' and on the type of cation ordering in the structure. In recent years, there have appeared a large number of publications dealing with experimental and theoretical investigations of the compounds belonging to the family of double perovskites [1–5]. In their recent work, Franco et al. [2] synthesized new double perovskites LaPb*Me*SbO$_6$, where Me^{2+} = Mn^{2+}, Co^{2+}, and Ni^{2+}. The X-ray diffraction analysis of the synthesized compounds demonstrated that the unit cell of the studied samples has the monoclinic symmetry space group $P2_1/n$, cations La and Pb are completely disordered, and cations Me^{2+} and Sb are ordered in the structure of the rock salt. All the studied samples undergo antiferromagnetic phase transitions at the Néel temperatures T_N = 8, 10, and 17 K for Me^{2+} = Mn^{2+}, Co^{2+}, and Ni^{2+}, respectively.

In this paper, we have presented the results of ab initio calculations of the ferroelectric, electronic, and magnetic properties of the completely ordered double perovskites LaPb*Me*SbO$_6$, where Me^{2+} = Mn^{2+}, Fe^{2+}, Co^{2+}, and Ni^{2+}. We have assumed that the ordering of cations in the *A* position should lead to the appearance of ferroelectric properties in the studied compounds, but should not significantly affect the magnetic properties.

2. COMPUTATIONAL TECHNIQUE

The calculations were carried out in the framework of the density functional theory using the Perdew–Burke–Ernzerhof (PBE) exchange–correlation functionals in the generalized gradient approximation (GGA) implemented in the VASP software package [6, 7]. In the calculation, we used the GGA + *U* method in the Dudarev approximation [8], where the value of $U' = U - J$ (here, *U* is the Hubbard repulsion at a single site and *J* is the intraatomic Hund

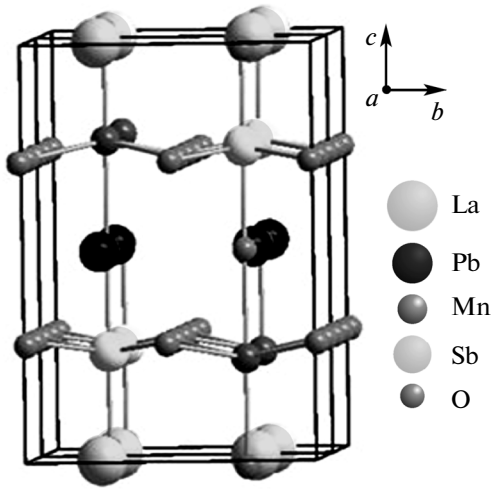

Fig. 1. Structure of the high-symmetry phase *P*4/*mmn*.

Table 1. Optimized lattice parameters (Å) of the high-symmetry phase

Lattice parameter	$LaPbMnSbO_6$	$LaPbFeSbO_6$	$LaPbCoSbO_6$	$LaPbNiSbO_6$
a	5.78	5.78	5.67	5.67
c	8.24	8.06	8.24	8.09

Table 2. Optimized coordinates of the ions in the high-symmetry phase

Atom	WP	$LaPbMnSbO_6$	$LaPbFeSbO_6$	$LaPbCoSbO_6$	$LaPbNiSbO_6$
La	2*a*	0.7500	0.750	0.750	0.750
		0.2500	0.250	0.250	0.250
		0.0000	0.000	0.000	0.000
Pb	2*b*	0.7500	0.750	0.750	0.750
		0.2500	0.250	0.250	0.250
		0.5000	0.500	0.500	0.500
Me^{2+}	2*c*	0.2500	0.250	0.250	0.250
		0.2500	0.250	0.250	0.250
		0.2564	0.255	0.252	0.251
Sb	2*c*	0.2500	0.250	0.250	0.250
		0.2500	0.250	0.250	0.250
		0.7558	0.754	0.752	0.751
O_1	8*j*	0.4927	0.492	0.497	0.496
		0.4927	0.492	0.497	0.496
		0.7715	0.770	0.770	0.769
O_2	2*c*	0.2500	0.250	0.250	0.250
		0.2500	0.250	0.250	0.250
		−0.0027	0.002	−0.005	−0.001
O_3	2*c*	0.2500	0.250	0.250	0.250
		0.2500	0.250	0.250	0.250
		0.5140	0.507	0.512	0.506

WP are the Wyckoff positions.

exchange) was varied for different compounds under the condition providing for a better coincidence of the calculated Néel temperatures with the experimental values ($U'_{Mn} = 5$ eV, $U'_{Fe} = 4$ eV, $U'_{Co} = 3$ eV, $U'_{Ni} = 2$ eV). All the calculations were performed taking into account the spin polarization. For structural calculations, we used the supercell $\sqrt{2}\,a \times \sqrt{2}\,a \times 2a$ (where a is the lattice parameter of the perovskite) containing 20 atoms (Fig. 1). For calculations of the exchange constants in the low-symmetry phase, we used the supercell $2a \times 2a \times 2a$ containing 40 atoms. The interaction of the next-nearest neighbors was taken into account using the supercell $4a \times 2a \times 2a$ containing 80 atoms. The Monkhorst–Pack k-point mesh was chosen to be $6 \times 6 \times 6$. The lattice parameters and ionic coordinates were optimized until the residual forces at the ions became less than 0.02 eV/Å. The exchange constants of the Heisenberg Hamiltonian were calculated from the difference in the energies between three magnetic configurations.

3. RESULTS AND DISCUSSION

As was mentioned in the Introduction, the experimental samples have the monoclinic symmetry space group $P2_1/n$, cations La and Pb are disordered, and cations Me^{2+} and Sb are ordered in the structure of the rock salt (checkerboard ordering). In this work, we investigated the double perovskites $LaPbMeSbO_6$ with the simultaneous ordering of both the cations A and the cations B. It is known from some studies [9, 10], double perovskites with the heterovalent substitution are predominantly characterized by a layered ordering of the cations A and A', along with a checkerboard ordering of the cations B and B' and, what is impor-

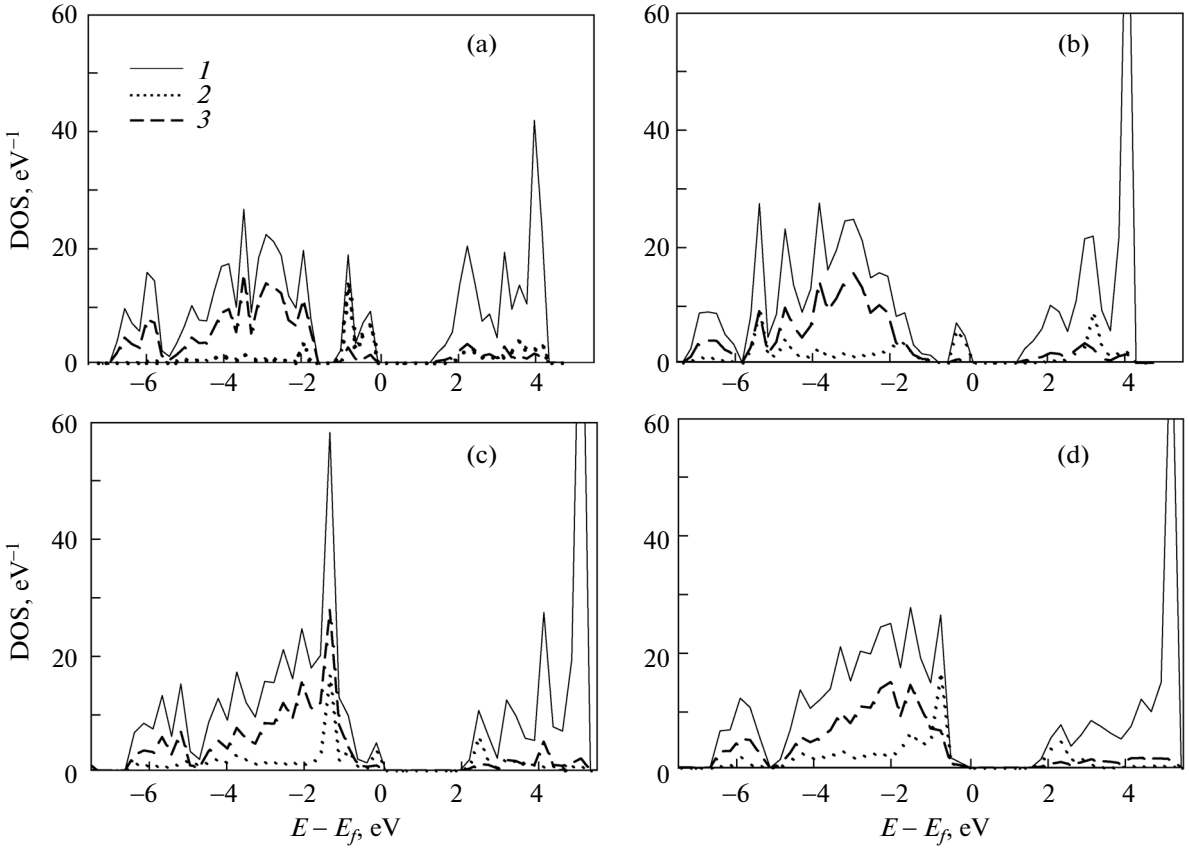

Fig. 2. Calculated total and partial densities of states in the high-symmetry phase: (a) $LaPbMnSbO_6$, (b) $LaPbFeSbO_6$, (c) $LaPbCoSbO_6$, and (d) $LaPbNiSbO_6$. (*1*) Total density of states, (*2*) *d* states of the metal (*Me*), and (*3*) *p* state of oxygen. Zero on the energy scale corresponds to the Fermi energy.

tant, this type of ordering can lead to a low-symmetry polar phase. It should be noted that, in our work, the calculations of the experimentally obtained partially ordered structures were performed using the virtual crystal approximation in the model of polarizable ions [11]. The calculation of the lattice dynamics demonstrated that all the studied compounds have unstable modes in the symmetric points Γ and *X* of the Brillouin zone, and the maximum (in magnitude) instabilities are associated with the "rotation" of the oxygen octahedra (for example, the corresponding frequencies of the unstable modes for $LaPbMnSbO_6$ are as follows: $\omega_\Gamma = 140i$ and $\omega_X = 135i$). The condensation of these modes actually leads to a nonpolar ground state with the symmetry space group $P2_1/n$ in accordance with the experiment.

Let us first consider the structural phase transition in the double perovskites under investigation. The high-symmetry nonpolar phase with a layered ordering of the cations *A* and a checkerboard ordering of the cations *B* has the tetragonal symmetry space group $P4/mmn$. We assume that all structural phase transitions, including the ferroelectric phase transition, occur in the paramagnetic phase, because the experimental Néel temperatures (see Introduction) are sufficiently small. The calculation of the electron density of states (DOS) in the high-symmetry phase without inclusion of the spin polarization demonstrated that all the compounds under consideration are metals. Therefore, further, we will present the results of the calculations of the structure and lattice dynamics with the inclusion of the spin polarization upon antiferromagnetic ordering of Me^{2+} magnetic moments ($Me^{2+} = Mn^{2+}$, Fe^{2+}, Co^{2+}, Ni^{2+}).

The complete geometry optimization of the lattice in the tetragonal phase leads only to small displacements of the oxygen ions along free coordinates. The optimized lattice parameters and atomic coordinates are presented in Tables 1 and 2, respectively.

The total and partial densities of states as functions of the energy are shown in Fig. 2. The zero energy corresponds to the Fermi energy calculated for each compound. The result of the spin-polarized calculation demonstrates that, in the high-symmetry tetragonal phase, all the compounds are insulators with a band gap of approximately 1.5–1.8 eV. The valence band is predominantly occupied by Me^{2+} *d* electrons and O^{2-} *p* electrons. The large peak in the conduction band is

Table 3. Vibrational frequencies (cm^{-1}) at the center of the Brillouin zone for the high-symmetry phase (the unstable modes are denoted by the index *i*; the degeneracy of the mode is given in parentheses)

$LaPbMnSbO_6$	$LaPbFeSbO_6$	$LaPbCoSbO_6$	$LaPbNiSbO_6$	$LaPbMnSbO_6$	$LaPbFeSbO_6$	$LaPbCoSbO_6$	$LaPbNiSbO_6$
152.9*i*	148.2*i*	143.2*i*(2)	136.2*i*(2)	262.9	233.2(2)	230.2(2)	225.2(2)
134.3(2)	144.6*i*(2)	138.6*i*	127.6*i*	274.3(2)	239.4(2)	238.4(2)	246.4(2)
116.1*i*(2)	108*i*(2)	94.2*i*(2)	89.2*i*(2)	299.6(2)	251.2	251.2	260.2
62.0*i*(2)	54.9*i*(2)	38.1*i*(2)	30.1*i*(2)	303.1(2)	290.9(2)	287.9(2)	263.9(2)
54.7*i*	47.1*i*	47.0*i*	34.0*i*	319.4	305.3(2)	303.3(2)	314.3(2)
32.2	42.2	24.4	21.4	330.0(2)	320.5	325.5(2)	341.5(2)
35.2	46.1	38.0	35.0	341.4	333.9(2)	361.9	387.9
49.4	52.3(2)	45.2	47.2	375.1(2)	369.6(2)	374.6(2)	391.6(2)
65.7(2)	62.7	55.2(2)	51.2(2)	581.9(2)	373.1	418.1(2)	448.1(2)
77.9	73.0	64.1	61.1	405.2	399.4(2)	569.4	573.4
85.8(2)	76.0(2)	76.4(2)	76.4(2)	456.2	424.0	577.0	582.0
95.8	79.5	79.4	73.4	516.8(2)	572.9(2)	579.9(2)	594.9(2)
141.3(2)	139.1(2)	135.7(2)	126.7(2)	594.2(2)	588.2(2)	588.2(2)	601.2(2)
147.0	143.6	138.8(2)	128.8(2)	607.6	657.2	637.2	646.2
151.2(2)	150.9(2)	153.7	154.7	610.5(2)	660.8	642.8	654.8
165.4	194	183.1	178.1	614.2	662.2(2)	667.2(2)	685.2(2)
178.2	198.8(2)	199.0(2)	201.0(2)	631.2(2)	663.6(2)	668.6(2)	674.6(2)
183.9(2)	205.3(2)	209.8(2)	212.8(2)	664.3	702.5	672.5	695.5
198.2(2)	208.8	212.8	215.8	685.2	720.2	739.2	749.2
229.3	224.3(2)	214.3(2)	218.3(2)	711.0	740.0	745.0	751.0
234.5(2)	232.0	222.0	221.0				

Table 4. Frequencies of the most unstable vibrational modes (cm^{-1}) in the tetragonal phase (the unstable modes are denoted by the index *i*)

Unstable mode	$LaPbMnSbO_6$	$LaPbFeSbO_6$	$LaPbCoSbO_6$	$LaPbNiSbO_6$
E_u	116*i*	108*i*	94*i*	89*i*
E_g	134*i*	144*i*	143*i*	136*i*
A_{1u}	152*i*	148*i*	138*i*	127*i*

Table 5. Optimized lattice parameters (Å) of the low-symmetry phase

Lattice parameter	$LaPbMnSbO_6$	$LaPbFeSbO_6$	$LaPbCoSbO_6$	$LaPbNiSbO_6$
a	5.81	5.78	5.78	5.7
b	5.79	5.69	5.73	5.67
c	8.3	8.11	8.3	8.17

associated with the unoccupied La *f* states. For all the studied compounds, there is a sharp peak in the valence band near the Fermi energy, which is associated with the Me^{2+} t_{2g} states. This peak is especially pronounced in the $LaPbMnSbO_6$ compound. For compounds with Fe, Co, and Ni, this peak gradually decreases and shifts deep into the valence band. The unoccupied e_g states are located near the Fermi level in the conduction band.

For the optimized structure, we calculated the lattice dynamics. The vibrational frequencies at the center of the Brillouin zone are presented in Table 3. As

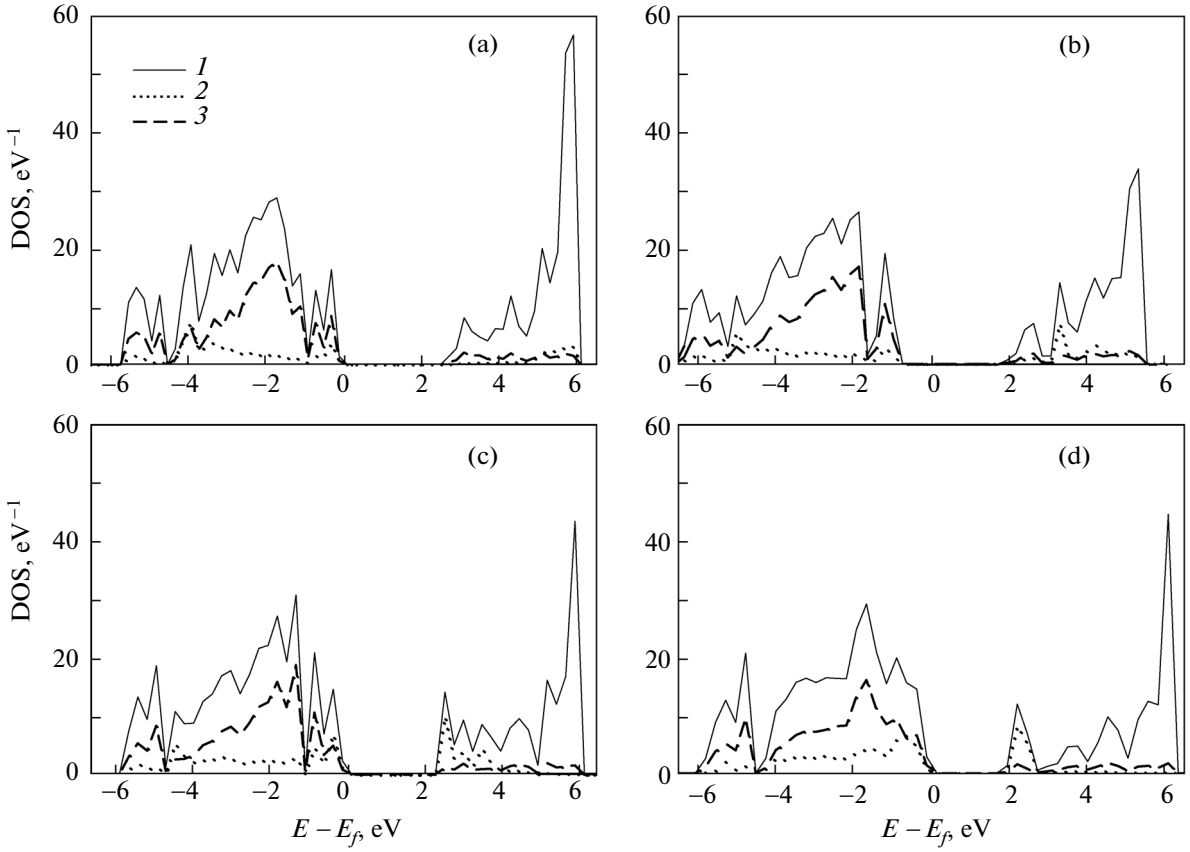

Fig. 3. Calculated total and partial densities of states in the low-symmetry phase: (a) $LaPbMnSbO_6$, (b) $LaPbFeSbO_6$, (c) $LaPbCoSbO_6$, and (d) $LaPbNiSbO_6$. Curves *1–3* are the same as in Fig. 2. Zero on the energy scale corresponds to the Fermi energy.

can be seen from Table 3, all the compounds have the unstable modes at the center of the Brillouin zone. The most unstable vibrational modes are associated with the rotation (mode A_{1u}), with the inclination (mode E_g) of oxygen octahedra, and with the polar distortion of the structure (mode E_u). The frequencies of the corresponding modes are listed in Table 4. It should be noted that the maximum displacements in the eigenvector of the E_u mode are observed in the lead and oxygen ions. For example, the x component of the eigenvector of the polar mode for the $LaPbMnSbO_6$ compound in the tetragonal phase with two molecules per cell has the form (–0.008, –0,008, 0.1, 0.1, 0.03, 0.03, 0.01, 0.01, –0.03, –0.03, –0.03, –0.03, –0.07, –0.68, –0.03, –0.03, –0.03, –0.03, –0.07, –0.68).

Following [12] and using the Bilbao crystallographic server [13, 14], we found that the condensation of any two of the three unstable modes leads to the monoclinic phase with the polar symmetry group $P2_1$. The structure of the low-symmetry phase was completely optimized. The obtained lattice parameters and atomic coordinates are presented in Tables 5 and 6, respectively.

The lattice parameters are found to be close to the lattice parameters obtained by Blanco et al. [15], who studied the related compounds $BaLaXSbO_6$ (X = Mn, Co, and Ni). The calculation of the lattice dynamics revealed the absence of unstable modes in the phonon spectra of low-symmetry monoclinic phase for all the compounds under investigation. Therefore, this monoclinic phase is the ground state for double perovskites with the considered type of cation ordering. It should be noted that, in the experimentally studies structures, the cations A and A' are disordered, which corresponds to the structure of the double perovskite $A_2BB'O_6$. It is known that, in many compounds with this structure, the low-symmetry stable phase has the nonpolar symmetry group $P2_1/n$ [16, 17], which is associated with the rotation of oxygen octahedra. This distortion suppresses the ferroelectric properties, which is actually observed in the experiment. It should be noted that, in the studied compounds, the antiferrodistorsive distortions by themselves also lead to the suppression of a ferroelectric instability (for example, in the phase where the distortions are related only to the "rotation" of $B'O_6$ octahedra, the calculated value of the frequency of the unstable polar mode is 73 cm^{-1}), but the

Table 6. Optimized coordinates of the ions in the low-symmetry phase

Atom	WP	$LaPbMnSbO_6$	$LaPbFeSbO_6$	$LaPbCoSbO_6$	$LaPbNiSbO_6$
La	2*a*	0.75547	0.75280	0.75372	0.25374
		0.54068	0.53233	0.53559	0.53274
		0.49893	−0.0013	−0.0011	0.49883
Pb	2*a*	0.74282	0.74208	0.74325	0.24250
		0.53395	0.51315	0.51826	0.52317
		−0.0023	0.49890	0.49833	−0.0019
Me	2*a*	0.75272	0.75136	0.75135	0.25101
		0.01313	0.00561	0.00917	0.00788
		0.24411	0.75100	0.74669	0.24876
Sb	2*a*	0.74805	0.75109	0.75037	0.25016
		0.00122	0.00297	0.00228	0.00234
		0.74601	0.25151	0.24965	0.75015
O_1	2*a*	0.53677	0.53367	0.53334	0.03489
		0.69381	0.70826	0.70455	0.70568
		0.22892	0.73105	0.73020	0.23163
O_2	2*a*	−0.0155	−0.0183	−0.0193	0.48169
		0.28919	0.28081	0.28286	0.28078
		0.31310	0.80370	0.80497	0.30453
O_3	2*a*	0.04285	0.03034	0.03782	0.53174
		0.76900	0.77190	0.76767	0.77091
		0.30296	0.79913	0.80140	0.29863
O_4	2*a*	0.43948	0.45259	0.44326	−0.0488
		0.20768	0.21291	0.21319	0.21089
		0.23287	0.73402	0.73180	0.23489
O_5	2*a*	0.33324	0.32088	0.32534	0.82093
		0.48255	0.49262	0.48696	0.49083
		0.49306	−0.0039	−0.0028	0.49514
O_6	2*a*	0.18712	0.1869	0.1860	0.6911
		0.47335	0.48400	0.48402	0.47933
		0.01681	0.50663	0.50743	0.00891

WP are the Wyckoff positions.

Table 7. Calculated values of the effective Born charges (electron charge units) and the spontaneous polarization ($\mu C/cm^2$)

Parameter	$LaPbMnSbO_6$	$LaPbFeSbO_6$	$LaPbCoSbO_6$	$LaPbNiSbO_6$
Z_{La}	4.50	4.52	4.46	4.47
Z_{Pb}	3.92	3.90	3.95	3.95
Z_{Me}	2.50	2.24	2.3	2.48
Z_{Sb}	4.25	4.3	4.45	4.46
Z_{O_1}	−2.54	−2.54	−2.56	−2.61
Z_{O_2}	−2.27	−2.19	−2.22	−2.27
Z_{O_3}	−2.68	−2.61	−2.67	−2.75
P	30	28	26	25

Table 8. Calculated energies of different magnetic configurations (eV) and magnetic moments of the Me^{2+} ions (in Bohr magnetons)

Parameter	$LaPbMnSbO_6$	$LaPbFeSbO_6$	$LaPbCoSbO_6$	$LaPbNiSbO_6$
E_F	138.6542	134.0642	130.1041	128.2900
E_{AF1}	138.6713	134.0883	130.1362	128.3335
E_{AF2}	138.6684	134.0855	130.1324	128.3284
μ	4.6	3.7	2.6	1.7

Table 9. Exchange interaction constants (eV)

Exchange constant	$LaPbMnSbO_6$	$LaPbFeSbO_6$	$LaPbCoSbO_6$	$LaPbNiSbO_6$
J_1	0.0001	0.0012	0.0015	0.002
J_2	−0.00005	−0.0001	−0.00014	−0.0002

Table 10. Calculated and experimental values [2] of the Néel temperature and the Curie–Weiss temperature (K)

Temperature	$LaPbMnSbO_6$	$LaPbFeSbO_6$	$LaPbCoSbO_6$	$LaPbNiSbO_6$
T_N (calc.)	18	21	24	37
T_{CW} (calc.)	−84	−86	−96	−124
T_N (exp.)	8	–	10	17
T_{CW} (exp.)	−57	–	−62	−119

combined effect of the modes associated with the rotation and inclination of the oxygen octahedra "pulls" the spontaneous polarization, which appears as the secondary order parameter.

The total and partial densities of states in the low-symmetry phase with the antiferromagnetic ordering of magnetic moments are shown in Fig. 3. The distortion of the structure leads to a small increase in the band gap (up to 2 eV) as compared to the high-symmetry phase. The peak in the density of states, which is associated with the Me^{2+} *d* electrons near the valence band edge, decreases. This is accompanied by an enhancement of the hybridization between the O *p* states and the Me^{2+} *d* states near the Fermi level.

The spontaneous polarization in the low-symmetry polar phase was calculated according to the formula

$$P_\alpha = \sum_{k,\beta} Z^*_{k,\alpha,\beta} \Delta u_{k,\beta}, \quad (1)$$

where $Z^*_{k,\alpha,\beta}$ are the calculated effective Born charges in the nonpolar phase (Table 7) and $\Delta u_{k,\beta}$ is the difference between the coordinates of the ions in the polar and nonpolar phases. The calculated polarization is oriented along the [100] direction. The obtained values of the spontaneous polarization are presented in Table 7. As can be seen from this table, the value of the spontaneous polarization is comparable to the polarization of a typical ferroelectric, such as $BaTiO_3$.

The presence of magnetic ions in the structure leads to the appearance of a magnetic ordering in addition to the electric polarization. The interactions responsible for the magnetic state of the low-symmetry phase can be evaluated from the interatomic exchange constants *J* with the calculated total energies of different magnetic configurations. The magnetic cations $Me^{2+} = Mn^{2+}$, Fe^{2+}, Co^{2+}, and Ni^{2+} are ordered in the face-centered cubic (fcc) lattice. Therefore, each atom has twelve nearest neighbors and six next-nearest neighbors. For the antiferromagnetic ordering, it is convenient to separate the face-centered cubic lattice into eight sublattices [18]. In this case, each atom has two nearest neighbors from six sublattices and six next-nearest neighbors from the remaining one sublattice. In order to determine the exchange constants between the nearest and next-nearest neighbors, it is necessary to consider three magnetic configurations, namely, two antiferromagnetic (*AF*1 and *AF*2) and one ferromagnetic (*F*). The antiferromagnetic configurations used for the calculations are shown in Fig. 4, and the calculated energies of the configurations are given in Table 8.

The first type of antiferromagnetic ordering (the adjacent planes along the *z* axis have antiparallel directions of the spins) is the most energetically favorable for all the studied compounds. The magnetic moments for this type of magnetic ordering are presented in Table 8.

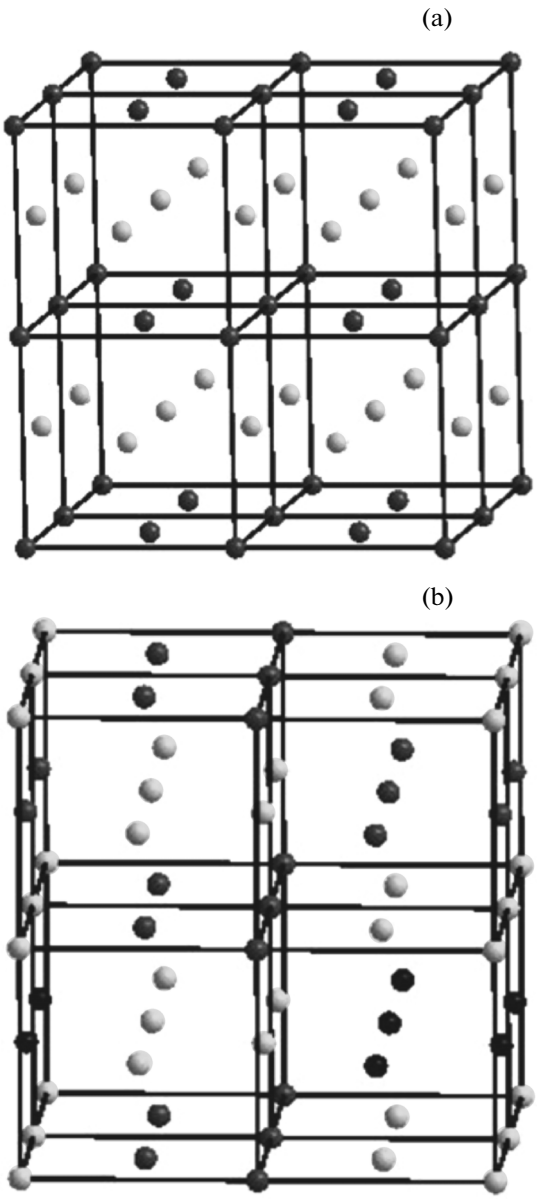

Fig. 4. Two types of antiferromagnetic ordering of magnetic moments in the face-centered cubic lattice, which are used for the calculation of the exchange constants: (a) *AF*1 configuration and (b) *AF*2 configuration (see text). Closed and open circles correspond to the antiparallel directions of the magnetic moments.

The constants J_1 and J_2 of the exchange interaction (between the nearest neighbor and next-nearest neighbors, respectively) were calculated using the classical Heisenberg Hamiltonian in the form

$$H = -\frac{1}{2}\sum_{i,j} J_{ij}\mathbf{S}_i\mathbf{S}_j, \qquad (2)$$

where J_{ij} is the constant of the exchange interaction between the ith and jth sites, and $\mathbf{S}_i$ and $\mathbf{S}_j$ are the effective values of the spin at the ith and jth sites, respectively.

The corresponding equations used to determine the exchange constants have the form

$$\begin{cases} E_F = -48J_1 - 24J_2 + E_0 \\ E_{AF1} = 16J_1 - 24J_2 + E_0 \\ E_{AF2} = 16J_1 - 8J_2 + E_0, \end{cases} \qquad (3)$$

where E_0 is the energy of the paramagnetic phase, and F, $AF1$, and $AF2$ are the energies of the ferromagnetic, type 1 antiferromagnetic, and type 2 antiferromagnetic configurations, respectively (as is shown in Fig. 4). The calculated values are presented in Table 9. The exchange constant J_1 corresponds to the antiferromagnetic ordering of the magnetic moments, whereas the exchange constant J_2 corresponds to the ferromagnetic ordering, and the value of J_2 is approximately one order of magnitude smaller than the value of J_1.

The Néel and the Curie–Weiss temperatures were estimated in the framework of the mean field approximation. The obtained Néel temperatures given in Table 10 are approximately two times higher than the experimental values; however, in the mean field approximation, this agreement is quite satisfactory. It should be noted that, recently, Karolak et al. [19] evaluated the Néel temperature of the double perovskite La_2NiTiO_6 with a checkerboard ordering of cations Ni and Ti. The obtained temperature $T_N = 50$ K (the experimental value is 25 K) agrees well with the result of our work. Moreover, the calculation gave the experimentally observed increase in the temperature of the antiferromagnetic phase transition with a change in the composition from Mn^{2+} to Ni^{2+}. The obtained Curie–Weiss temperatures were also found to be close to the experimental values. The low values of the Néel temperatures are most likely associated with the complex indirect exchange *Me*–O–Sb–O–*Me* in the studied compounds.

4. CONCLUSIONS

Within the framework of the density functional theory implemented in the VASP software package, we performed a theoretical investigation of the ferroelectric and magnetic properties of the double perovskites $LaPbMeSbO_6$ (Me^{2+} = Mn^{2+}, Fe^{2+}, Co^{2+}, Ni^{2+}). We considered the case of a layered ordering of cations *A* and a checkerboard ordering of cations *B*. The results of the calculation of the electron density of states with the inclusion of the spin polarization indicate that all the studied compounds are insulators. The spectrum of lattice vibrations of the high-symmetry tetragonal phase exhibits instabilities associated with the polar and antiferrodistorsive distortions of the lattice. The condensation of the most unstable modes leads to the

formation of a low-symmetry polar phase, for which we estimated the spontaneous polarization. The calculation of different magnetic configurations in the low-symmetry phase demonstrated that, in the magnetic ground state, the magnetic moments are antiferromagnetically ordered with opposite spin directions in adjacent planes along the [001] direction. The results of the calculation of the Néel and Curie–Weiss temperatures are in satisfactory agreement with the experimental data. The obtained temperatures are rather small due to the complex exchange between the magnetic ions. Thus, we can assume that the ordering of the cations A' and B' in the double perovskites $LaPbMeSbO_6$ leads to the coexistence of the magnetic and ferroelectric order parameters in these compounds.

ACKNOWLEDGMENTS

This study was supported by the Russian Foundation for Basic Research (project no. 12-02-00025-a) and the Council on Grants from the President of the Russian Federation in Support of the Leading Scientific Schools (grant no. NSh-924-2014.2). Calculations were performed on supercomputers of the National Research Centre "Kurchatov Institute" (Moscow, Russia).

REFERENCES

1. D. Serrate, J. M. De Teresa, and M. R. Ibarra, J. Phys.: Condens. Matter **19**, 023201 (2007).
2. D. G. Franco, R. E. Carbonio, and G. Nieva, IEEE Trans. Magn. **49**, 4594 (2013).
3. G. Vaitheeswaran, V. Kanchana, and A. Delin, Appl. Phys. Lett. **86**, 032513 (2005).
4. D. Stoeffler and C. Etz, J. Phys.: Condens. Matter **18**, 11291 (2006).
5. S. Gong, P. Chen, and B. G. Liu, J. Magn. Magn. Mater. **349**, 74 (2014).
6. G. Kresse and J. Furthmuller, Phys. Rev. B: Condens. Matter **54**, 11 169 (1996).
7. J. P. Perdew, K. Burke, and M. Ernzerhof, Phys. Rev. Lett. **77**, 3865 (1996).
8. S. L. Dudarev, G. A. Botton, S. Y. Savrasov, C. J. Humphreys, and A. P. Sutton, Phys. Rev. B: Condens. Matter **57**, 1505 (1998).
9. G. King and P. M. Woodward, J. Mater. Chem. **20**, 5785 (2010).
10. T. Fukushima, A. Stroppa, S. Picozza, and J. M. Perez-Mato, arXiv:1104.5099v1 [cond-mat.mtr-sci]r
11. E. G. Maksimov, V. I. Zinenko, and N. G. Zamkova, Phys.—Usp. **47** (11), 1075 (2004).
12. N. G. Zamkova, V. S. Zhandun, and V. I. Zinenko, Phys. Status Solidi B **250**, 1888 (2013).
13. D. Oronbegoa, C. Capillas, M. I. Aroyo, and J. M. Perez-Mato, J. Appl. Crystallogr. **42**, 820 (2009).
14. J. M. Perez-Mato, D. Orobengoa, and M. I. Aroyo, Acta Crystallogr., Sect. A: Found. Crystallogr. **66**, 558 (2010).
15. M. C. Blanco, J. M. De Paoli, S. Ceppi, G. Tirao, V. M. Nassif, J. Guimpel, and R. E. Carbonio, J. Alloys Compd. **606**, 139 (2014).
16. W. Prellier, V. Smolyaninova, A. Biswas, C. Galley, R. L. Greene, K. Ramesha, and J. Gopalakrishnan, J. Phys.: Condens. Matter **12**, 965 (2000).
17. L.T. Corredor, D.A. Landínez Téllez, J. L. Pimentel, Jr., P. Pureur, and J. Roa-Rojas, J. Mod. Phys. **2**, 154 (2011).
18. J. S. Smart, *Effective Field Theories of Magnetism* (Saunders, London, 1966; Mir, Moscow, 1968).
19. M. Karolak, M. Edelmann, and G. Sangiovanni, arXiv:1407.2255v1 [cond-mat.mtr].

Translated by O. Borovik-Romanova